WORLD JOURNAL OF PHARMACEUTICAL RESEARCH
Coden USA: WJPRAP Impact Factor 8.453
Volume 14, Issue 21, 1410-1430. Research Article ISSN 2277–7105

DEVELOPMENT OF PACLITAXEL-LOADED SOLID LIPID NANOPARTICLES USING A TEMPERATURE-MODULATED SOLIDIFICATION TECHNIQUE FOR SUSTAINED DRUG DELIVERY APPLICATIONS

Ameya Abhay Deshpande*[1,2], Junkyu Shin[1], Steven Gollmer[3], Elisha Injeti[4], Jerry Nesamony[1]

[1]College of Pharmacy and Pharmaceutical Sciences, the University of Toledo, Health Science Campus, Toledo, OH 43614.
[2]Department of Product Development, Catalent Pharma Solutions, San Diego, CA.
[3]Department of Science and Mathematics, Cedarville University, Cedarville, OH.
[4]Department of Pharmaceutical Sciences, School of Pharmacy, Cedarville University, Cedarville, OH.

Article Received on 24 October 2025,
Article Revised on 30 October 2025,
Article Published on 01 November 2025,

https://doi.org/10.5281/zenodo.17540411

***Corresponding Author**
Ameya Abhay Deshpande
College of Pharmacy and Pharmaceutical Sciences, the University of Toledo, Health Science Campus, Toledo, OH 43614.

How to cite this Article: Ameya Abhay Deshpande*1,2, Junkyu Shin1, Steven Gollmer3, Elisha Injeti4, Jerry Nesamony1 (2025). Development of Paclitaxel-Loaded Solid Lipid Nanoparticles Using A Temperature-Modulated Solidification Technique For Sustained Drug Delivery Applications. World Journal of Pharmaceutical Research, 14(21), 1410–1430.

1. ABSTRACT

Objective: The objective of this research was to formulate, characterize, and evaluate paclitaxel-loaded solid lipid nanoparticles (SLNs) using a temperature-modulated solidification technique, with the goal of achieving sustained drug delivery. **Methods:** SLNs were prepared by incorporating paclitaxel into glyceryl monostearate (GMS) with Tween 80 as an emulsifier, using a temperature-modulated solidification process. Particle size and morphology were assessed via dynamic light scattering (DLS), transmission electron microscopy (TEM), and atomic force microscopy (AFM). Zeta potential analysis was conducted to evaluate physical stability. The solid-state characteristics were investigated through differential scanning calorimetry (DSC), powder X-ray diffraction (P-XRD), and Fourier transform infrared spectroscopy (ATR-FTIR). Entrapment efficiency was quantified, and in-vitro drug release studies were performed to determine the release kinetics. **Results:** The nanoparticles exhibited a spherical shape and nanometer size range. Zeta potential measurements indicated

physical stability owing to a negative surface charge. AFM revealed minimal aggregation and uniformity in shape. DSC, P-XRD, and ATR-FTIR analyses confirmed the successful entrapment of paclitaxel within the lipid matrix and transformation of bulk lipid to nanoparticles. The formulation demonstrated an entrapment efficiency of approximately 62%. In-vitro drug release studies showed sustained release of paclitaxel over a period of one week, following the Higuchi drug-release model. **Conclusion:** These findings highlight the potential of SLNs as an effective and physiologically safe drug delivery system for paclitaxel. The temperature-modulated solidification technique facilitated high drug entrapment and stable nanoparticle formation. The sustained release profile and compatibility with GRAS lipids underscore the feasibility of SLNs for improved chemotherapy applications. Further in-vivo studies and clinical evaluations are warranted to corroborate these promising results and advance the SLN platform for oncology therapeutics.

KEYWORDS: P-XRD, ATR-FTIR, DSC, nanometer, colloidal, sustained release.

2. INTRODUCTION

Paclitaxel (PCTL) is extracted from the bark of Taxus brevifolia and exerts its effects by interacting with tubulin. Studies indicate that PCTL-treated cells experience challenges in spindle assembly, cell division, and chromosome segregation. Furthermore, PCTL functions to stabilise microtubules and safeguard them against disassembly.[1] PCTL is used for the treatment of several types of tumors, including ovarian cancer, breast cancer, lung cancer, head and neck cancers, esophageal cancer, bladder cancer, endometrial cancer, hematological malignancies, and pediatric cancers.[2] PCTL exhibits low water solubility, which presents challenges in creating suitable pharmaceutical formulations. The initial clinical formulation employed a combination of Chremophor EL and ethanol as solvents for solubilizing PCTL. Studies have indicated that Cremophor EL is associated with side effects including hypersensitivity, nephrotoxicity, and neurotoxicity. As a result, various researchers are working on developing Cremophor EL-free formulations containing PCTL.[3] Lipid-based delivery systems, including solid lipid nanoparticles (SLNs), have garnered significant attention in pharmaceutical formulation in recent years, owing to their capability for transporting and solubilizing lipophilic drugs.[4] Solid lipid nanoparticles (SLNs) have emerged as promising colloidal drug delivery systems, combining the advantages of traditional formulations while mitigating many of their limitations. SLNs are composed of solid lipids that are cost-effective and classified as generally recognized as safe (GRAS),

ensuring physiological safety. Furthermore, they offer enhanced physical stability, consistent reproducibility, and can be manufactured at relatively low costs.[5, 6 and 7]

This study involved the development of solid lipid nanoparticles designed to transport paclitaxel to specific sites with sustained release. Paclitaxel was loaded into SLNs prepared using glyceryl monostearate (GMS) as the lipid and tween 80 as an emulsifier. The potential of SLNs for paclitaxel delivery was assessed through characterization of properties including particle size, shape, drug entrapment efficiency, solid-state characteristics, and drug release.[8]

3. MATERIALS AND METHODS

3.1. Materials

Glyceryl Monostearate (GMS) was sourced from PCCA (Houston, TX). Tween 80, acetonitrile (HPLC grade), and sterilized phosphate buffer solution (PBS) were procured from Fisher Scientific (Fair Lawn, NJ). Paclitaxel was supplied by TSZ CHEM. Anhydrous D-trehalose was obtained from Acros Organics (Fair Lawn, NJ).

3.2. Methods

3.2.1. Preparation of Paclitaxel-Loaded Solid Lipid Nanoparticles

The temperature-modulated solidification technique was used in preparation of solid lipid nanoparticles.[7, 9] An appropriate amount of Paclitaxel was mixed with 1 g of GMS in a small test tube and shaken at 75ºC, 1500 rpm for 48 hours using a temperature-controlled shaker (Multi-therm H5000-H, Benchmark Scientific Inc., NJ, USA). Subsequently, 2g of Tween 80 were incorporated into the mixture. The combined paclitaxel, Tween 80, and GMS were heated in a water bath (150 ml) at a temperature not exceeding 90ºC, with intermittent vortexing for 20 seconds every 5 minutes to ensure thorough mixing. At the same time, 150 ml of deionized water was heated to 80ºC. The molten mixture was added to the heated deionized water, and the resulting dispersion was placed in an ice bath and homogenized at 4000 rpm for 45 minutes. The homogenized dispersion was left on the bench for 30 minutes without disturbance. Subsequently, the dispersion was filtered using Amicon® Ultra Centrifugal filters (Ultracel®-100K) and centrifuged for 20 minutes. The residue was re-suspended in 40 ml deionized water and split into two equal portions. One portion was frozen at -80ºC with D-trehalose added, while the other was dialyzed in deionized water for 2 hours before being frozen at -80ºC with D-trehalose. Both portions were then lyophilized for 72 hours, weighed separately, and analyzed further.

3.2.2. Particle Size Analysis and Optimization Studies for Extracting the Surfactant from SLNs

The removal of surfactant from the final formulation is essential due to its potential hazardous effects on cellular systems. These evaluations were conducted using blank SLNs. As previously described in the formulation process, half of the non-lyophilized SLN dispersion underwent dialysis with a Fisherbrand® regenerated cellulose dialysis tubing (MWCO: 12,000–14,000) for two hours. Deionized water served as the medium during dialysis. Particle size analysis was conducted following each step of the formulation process, including homogenization, Amicon filtration, dialysis, and lyophilization. Additionally, particle size analysis was performed on the water utilized in dialysis. The measurements were obtained using dynamic light scattering (Nicomp 380 ZLS, CA, USA), equipped with a 100mW He-Ne laser at a wavelength of 658 nm and a photodiode array detector. All samples were transferred into disposable Durex® borosilicate glass culture tubes (Kimble Chase, Vineland, NJ) and analyzed at 23°C with a scattering angle of 90°. Particle size was reported as volume-weighted diameter. Data acquisition and analysis were conducted using Nicomp software.

3.2.3. Zeta Potential Analysis

The zeta potential of blank and paclitaxel-loaded SLNs was measured using dynamic light scattering (Nicomp 380 ZLS, CA, USA). One milligram of lyophilized sample was re-dispersed in 10 mL deionized water, vortexed at 3000 rpm for 5 minutes, then analyzed at 23°C and 14.06° using electrophoretic light scattering (ELS) mode. Data acquisition and analysis were performed with Nicomp software.

3.2.4. Imaging by Transmission Electron Microscopy (TEM).

5 mg of lyophilized blank and lyophilized PCTL-loaded SLNs were re-dispersed in 10 ml of deionized water and vortexed at 3000 rpm for 5 minutes. One drop of the sample was placed onto a Formvar/Carbon 400 mesh copper grid (Ted Pella, CA) and air dried for 24 hours at room temperature. Imaging was performed using a transmission electron microscope (Hitachi HD-2300A, Hitachi High Technologies America, IL, USA) operated at an acceleration voltage of 200 kV.

3.2.5. Atomic Force Microscopy (AFM).

Atomic force microscopy (AFM) imaging was performed using a Nanosurf Easyscan 2 AFM instrument, which included a cantilever and camera mounted on the Easyscan 2 head. The

instrument operated in dynamic force mode at a speed of 0.1 millimeters per second with a scan range of 25 micrometers. The results were processed by the Easyscan 2 controller and recorded via Easyscan 2 software. Samples obtained after various formulation steps (homogenization, amicon filtration, dialysis) were diluted with deionized water in a 1:10 v/v ratio; one drop from each was placed on separate mica disks and dried for 24 hours. Both blank lyophilized and PCTL-loaded lyophilized samples were resuspended in deionized water at a 1:10 w/v ratio; drops of each were similarly deposited on mica disks and allowed to dry for 24 hours. All dried samples were subsequently analyzed by AFM.

3.2.6. Differential Scanning Calorimetry (DSC).

Thermal behavior of pure GMS, pure PCTL, pure D+(-) trehalose, lyophilized blank, and lyophilized PCTL-loaded SLNs was tested using a Mettler Toledo DSC822e. Samples (5-8 mg) were sealed in 100 µl aluminum pans, with an empty pan as reference. Heating was performed at 10°C/min from 25 to 350°C under nitrogen, and thermograms were analyzed using Star-e software.

3.2.7. Powder X-ray Diffraction (pXRD).

X-ray scattering experiments were performed on pure GMS, pure paclitaxel base, as well as both lyophilized blank and PCTL-loaded SLNs. These measurements utilised a PANanlytical X-ray diffractometer (PANanlytical X'pert Pro, Tokyo, Japan), fitted with an X'Celerator high-speed detector and a CuKα source set at 45 kV and 40 mA. For analysis, samples were crushed and evenly packed into an aluminium holder using a glass slide. The instrument was operated in the continuous scanning speed of 4°/min over a 2θ range of 5° to 40° and the results were evaluated using the X-Pert data collector version 2.1 software.

3.2.8. Fourier Transform Infrared Spectroscopy (FTIR)

The spectra for pure GMS, pure PCTL base, as well as lyophilized blank and PCTL-loaded SLNs were recorded using a Thermo Scientific NICOLET iS5 Fourier Transform Infrared Spectrometer (iD3 ATR) equipped with a zinc-selenium crystal. Samples were placed directly on the crystal, and 16 scans were collected for each measurement. All spectra were acquired at a resolution of 4 cm–1.

3.2.9. Drug Entrapment Efficiency

Approximately 5 mg of lyophilized PCTL-loaded solid lipid nanoparticles (SLNs), formulated with 50 mg, 75 mg, and 100 mg of PCTL, respectively, were dissolved in 10 ml

of acetonitrile by vortexing at 3000 rpm for 2 minutes. The resulting solution was filtered through a 0.45 µm non-sterile, solvent-resistant polytetrafluoroethylene (PTFE) syringe filter (Fisherbrand, USA). 10 µl of the filtrate was used as the injection volume for analysis using reversed-phase high performance liquid chromatography (RP-HPLC) on a Waters HPLC e2695 separation module equipped with a photodiode array detector (Waters 2998). Chromatographic separation was performed using a Symmetry® C18 column (Waters, USA; 3.5 µm, 4.6 x 75 mm) as the stationary phase. An acetonitrile-water mixture in a ratio of 52:48 served as the mobile phase, delivered at an isocratic flow rate of 0.5 ml per minute with the column maintained at 30°C. Detection of PCTL was conducted at a wavelength of 227 nm. Data analysis was performed using Empower 3.0 software. Quantification was achieved via a calibration curve generated from pure PCTL in acetonitrile. Drug entrapment efficiency was calculated using the following formula.

$$\%\ \text{Drug entrapment efficiency} = \frac{\text{Practical PCTL content}}{\text{Theoretical PCTL content}} \times 100$$

3.2.10. In-vitro Drug Release Studies

100 mg of lyophilized PCTL-loaded SLNs were precisely weighed and dispersed in 1 ml of phosphate buffer solution (PBS, pH 7.4) contained within a sealed dialysis membrane (Spectra/Por® Dialysis Membrane, MWCO: 3500), with a molecular cut-off size of 3,500 Daltons. The dialysis membrane was submerged in a beaker holding 500 ml of 30% ethanol solution and maintained at 37°C ± 0.5°C in a water bath, covered with parafilm and subjected to magnetic stirring at 125 rpm. Samples (1 ml each) were withdrawn at predetermined intervals—15 minutes, 30 minutes, 1, 2, 4, 6, 8, 10, 12, 16, 20, 24, 30, 36, 42, 48, 60, 72, 96, 120, 144, and 168 hours—and replaced with fresh 30% ethanol solution. The quantity of PCTL released was determined using the previously described HPLC method.

3.2.11. Drug Release Data Modeling

To identify the optimal kinetic model describing the release profile of the formulated SLNs, the release data were evaluated using four distinct kinetic models: zero-order, first-order, Higuchi, and Korsmeyer-Peppas. The regression coefficient (R^2) served as the criterion for determining the best fit. Additionally, the release rate constant for each model was calculated.[11,12]

4. RESULTS AND DISCUSSIONS

4.1. Preparation of Paclitaxel Loaded Solid Lipid Nanoparticles

SLNs were synthesized using a temperature-modulated solidification method. This process entails carefully controlling the environmental temperature during concurrent solidification and formation of the lipid nanodispersion. Glyceryl monostearate and Tween 80 served as the lipid and surfactant, respectively, in the formulation. Application of shear forces through high-speed homogenization, followed by rapid cooling, facilitated SLN formation. Tween 80 reduced interfacial tension between the molten lipid and the aqueous phase as temperature decreased under controlled homogenization, thereby promoting SLN formation. The formulation was optimized by systematically varying parameters such as drug-to-lipid ratio, surfactant concentration, and emulsification duration. An increase in lipid concentration resulted in larger particle diameters, indicating that particle size is dependent on lipid content once a certain threshold is reached.[13] This procedure is simple and does not require organic solvents, thus demonstrating strong scalability potential. To minimize surfactant-induced toxicity in cellular and animal tissue models, the optimized formulation employs the lowest feasible surfactant concentration, maintaining a lipid-to-surfactant ratio of 1:2. Heydenreich et al investigated and compared the effect of three different purification techniques viz., ultrafiltration, ultracentrifugation and dialysis on cellular toxicity and physical stability of the SLNs.[14] In this formulation technique, ultracentrifugation was employed for purification and to enhance the physical stability of solid lipid nanoparticles (SLNs). Aqueous dispersions or suspensions tend to exhibit limited stability, which requires specific handling and storage conditions. Lyophilization is an effective method for converting aqueous dispersions into solid forms. Lyophilized powders exhibit enhanced stability.[15] Freeze drying introduces stresses that can destabilize nanoparticulate dispersions, resulting in aggregation and, in some cases, irreversible fusion of nanoparticles. To address this issue, cryoprotectants are added prior to freezing; these agents help protect the formulation from freezing stress.[16] Trehalose was selected as the cryoprotectant for the optimized formulation based on its effect on lyophilized SLN particle size after testing sucrose, mannitol, and trehalose. The final formulation used a 1:1 lipid-to-trehalose ratio.[7,9]

4.2. Particle Size Analysis and Optimization Studies for Extracting the Surfactant from SLNs

The particle size of blank SLNs was measured during each stage of the formulation process, including homogenization, amicon filtration, dialysis, and lyophilization. The results

indicated an increase in average particle diameter following amicon filtration and lyophilization, as shown in Table 1 and Figure 1. The observed increase in particle size following amicon filtration can be ascribed to the partial removal of surfactant (Tween 80) micelles from the formulation, which facilitates particle coalescence and subsequently shifts the average particle diameter toward a larger size range. An increase in particle diameter has been noted following lyophilization, even with the use of cryoprotectants.[17] An increase in particle diameter observed after lyophilization may result from using a smaller volume of redispersion media compared to the amount used during preparation, which increases SLN concentration and encourages interparticulate interactions that lead to aggregation and the formation of larger structures. Additionally, cryoprotectant can deposit on the surface of SLNs, further contributing to the overall increase in particle diameter.[7] The average particle diameter of paclitaxel-loaded SLNs was 419.5 ± 14.84 nm.

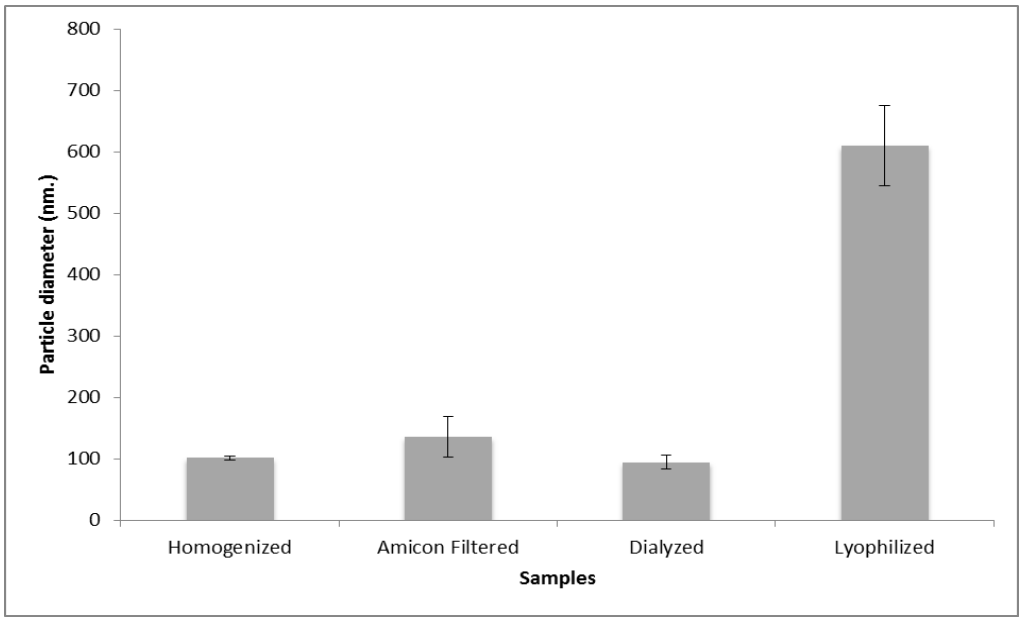

Figure 1: Particle size analysis of blank SLNs. The data represent the mean values (n=3) ± S.E.

Table 1: Particle sizes of different process samples. The data represent the mean values (n=3) ± S.E.

Process samples	Average particle diameter ± standard deviation (nm.)
Homogenized	101.46 ± 3.11
Amicon filtered	135.45 ± 33.16
Dialyzed	94.45 ± 10.90
Lyophilized	609.92 ± 64.88

As previously noted, surfactants have demonstrated toxic effects on cells and human tissues.[14] Therefore, an additional dialysis step was incorporated into the formulation procedure to minimize the concentration of surfactant. The medium employed during the dialysis phase was subsequently evaluated for particle size via dynamic light scattering (DLS) utilizing the Nicomp analysis mode, in order to accurately assess the predominant particle population. The particle sizes observed for the majority of the population ranged from 10 to 20 nm (Table 2), indicating micelles of surfactant tween 80 present in the dialysis media. This suggests the extraction of surfactant from the SLN dispersion.

Table 2: Dialysis media particle size analysis. The data represent the mean values (n=3) ± S.D.

	Peak-1		***Peak-2***		***Peak-3***	
	Particle diameter (nm.)	***Percentage***	***Particle diameter (nm.)***	***Percentage***	***Particle diameter (nm.)***	***Percentage***
Average ± Standard deviation	14.73 ± 3.46	88 ± 2.64	137.53 ±80.40	6.03 ±6.43	1791.5±1519.5	6.23 ± 3.72

4.3. Zeta Potential

Zeta potential analyses were conducted on both lyophilized blank and lyophilized PCTL-loaded SLNs (as shown in Table 3). The results indicated that all measured zeta potential values were negative, which can be attributed to the presence of glyceryl monostearate, a fatty acid ester.[18] Zeta potential is a key parameter for assessing the stability of colloidal dispersions.[19] A stable dispersion of particles can be achieved when the absolute value of zeta potential exceeds 30 mV, whether negative or positive, due to the repulsive forces generated by the surface electric charges present on particles within the dispersion.[5, 19, 20] Lower zeta potential values can cause interparticulate interaction, which may result in flocculation and coagulation. The measured zeta potential values for PCTL-loaded SLNs were over negative 30 mV, indicating that the SLNs exhibited physical stability.

Table 3: Zeta potential measurement results. The data represent the mean values (n=3) ± S.E.

	Lyophilized blank SLNs (mV)	**Lyophilized PCTL-loaded SLNs (mV)**
Zeta potential	-24.74 ± 0.17	-32.85 ± 0.33

4.4. TEM.

TEM was employed to observe the morphology of SLNs. This technique allows for the assessment of characteristics including particle size, shape, and internal structure of the nanoparticulate carrier system.[21] TEM images of lyophilized blank and lyophilized PCTL loaded SLNs were obtained (Figure 2). The TEM images indicated that the particles were spherical and had diameters in the nanometer range, consistent with DLS measurements. A core-shell structure with a drug-enriched core was also observed in the PCTL loaded SLNs.

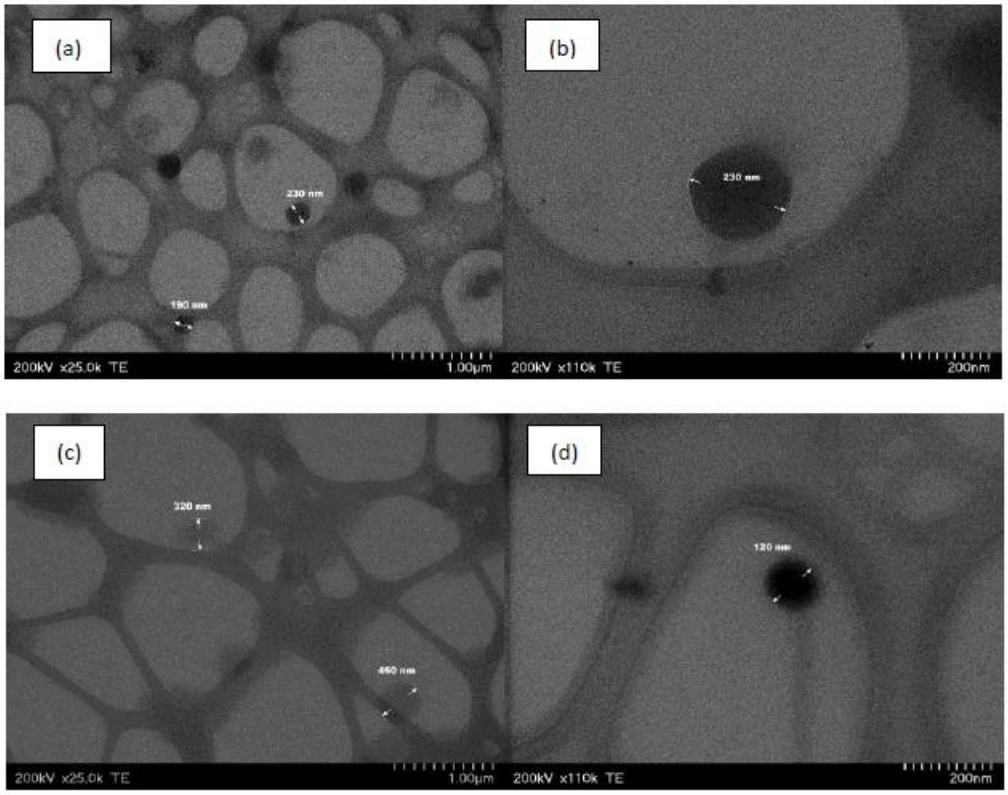

Figure 2: TEM images of (a) and (b) Lyophilized blank SLNs; (c) and (d) Lyophilized drug Paclitaxel loaded SLNs.

4.5. AFM

AFM was utilized to examine the morphology of SLNs throughout various stages of formulation, as well as to assess particle aggregation. Previous studies have indicated that AFM imaging can lead to observed clustering of SLNs, which in turn results in an apparent increase in particle size. This phenomenon is believed to be related to the sample preparation process for AFM, wherein incomplete drying may leave the samples hydrated, thereby promoting particle aggregation.[22] Similar results were observed during our analysis. The particle aggregation and particle sizes observed for lyophilized blank and lyophilized PCTL-

loaded SLNs were greater than those observed for the other process samples (Figure 3). This finding is consistent with the particle size data obtained through DLS and TEM analyses.

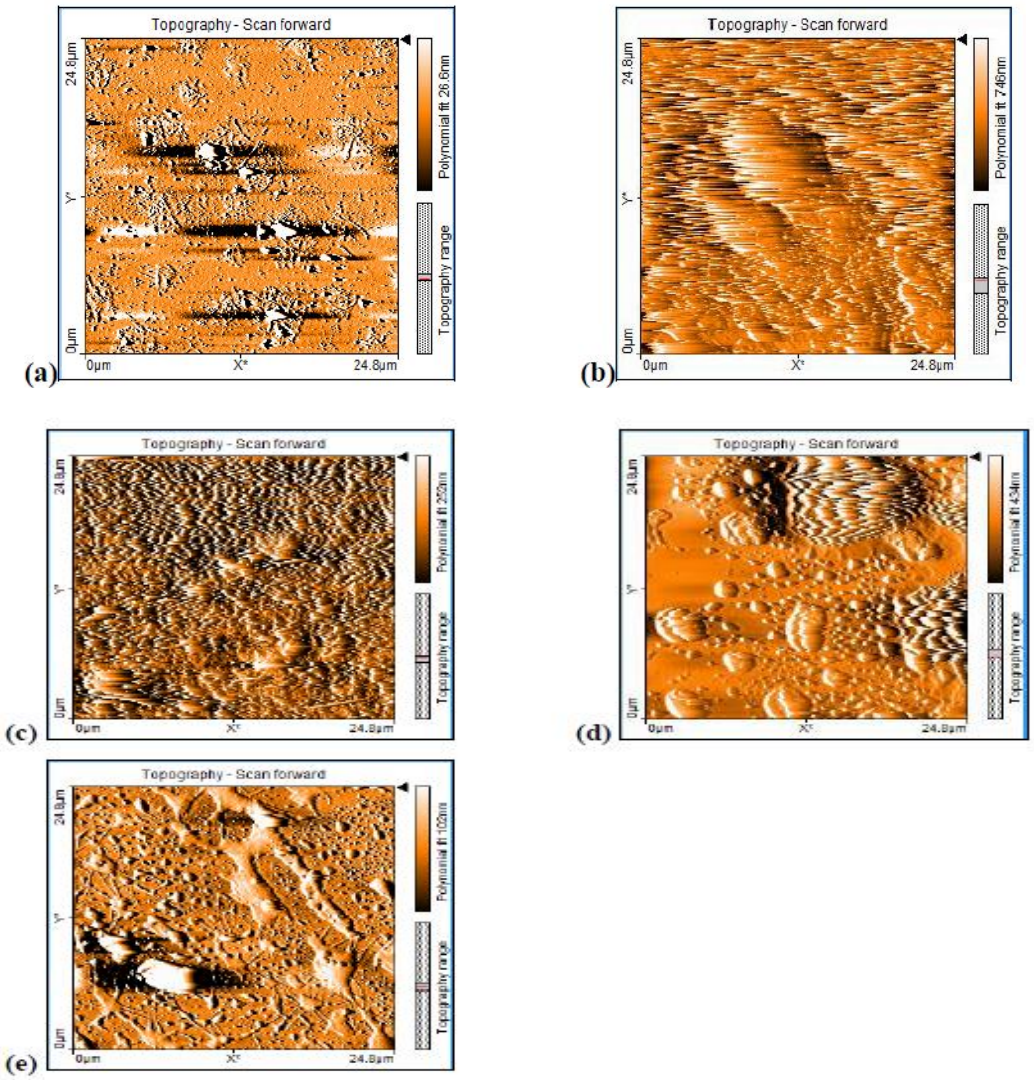

Figure 3: Shaded line-fit projection of AFM data for (a) blank homogenized sample, (b) blank amicon filtered sample (c) blank dialyzed sample, (d) blank lyophilized sample and (e) PCTL-loaded lyophilized sample of SLNs.

4.6. DSC

The temperature modulated solidification process involves melting the lipid and then allowing it to solidify as it cools, which causes the lipid to recrystallize. GMS displays an endothermic peak at a temperature of 71°C. SLNs prepared with this method melted near the same temperature but had melting peaks roughly 8°C lower than pure lipid, as shown in Figure 4. This behaviour indicates that the bulk lipid transforms into nanoparticles through a polymorphic shift from β'-modification to α-modification in its crystalline structure.[8, 23, 24]

The formation of nanoparticles results in a reduction in the degree of crystallinity, as well as a decrease in melting enthalpy. DSC analysis of pure PCTL exhibited an endothermic peak, with an onset temperature of 216.26 °C and a peak temperature of 223.68 °C.[25] An exothermic peak appeared right after the melting endothermic peak of PCTL, indicating its degradation.[26] The DSC thermogram of PCTL-loaded SLNs did not show a peak at or near 223.68 °C (Figure 4), which may suggest that the crystalline PCTL was either converted to an amorphous form within the SLNs or adequately dispersed into the melted GMS matrix.[27, 28]

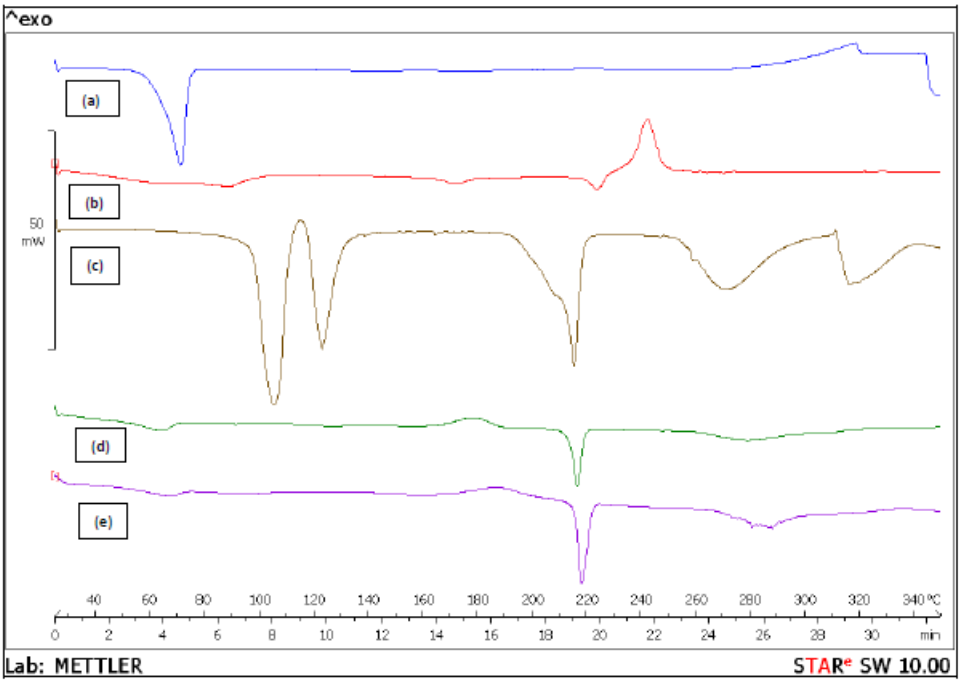

Figure 4: DSC thermograms for (a) pure GMS (b) pure PCTL (c) pure D (+) - trehalose (d) blank lyophilized SLNs (e) PCTL-loaded lyophilized SLNs.

4.7. pXRD

Powder X-ray diffraction was used to examine the solid-state properties of SLNs. Diffraction patterns for lyophilized PCTL-loaded and blank SLNs were compared to those for pure PCTL and pure GMS, respectively (Figure 5). Paclitaxel diffractogram exhibited sharp and high intensity peaks at 5.09, 5.14, 5.19, 9.60, 12.48, 37.71 and 43.94°. These peaks were either of very low intensity, less sharp, or completely absent in the diffractogram of PCTL-loaded SLNs. This demonstrates that paclitaxel is partially transformed into its amorphous form within the SLNs. Furthermore, it highlights the substantial drug loading capacity offered by the SLNs.[29] Pure GMS exhibited broad and high-intensity peaks at 2θ values of 19.54° and 23.46°. These characteristic peaks were also identified in the XRD patterns of both blank and PCTL-loaded SLNs, albeit with reduced intensities, indicating a decrease in the

crystallinity of GMS within the SLNs.[30] The XRD patterns of blank and PCTL-loaded SLNs showed no significant differences. These XRD findings are consistent with the data obtained from DSC.

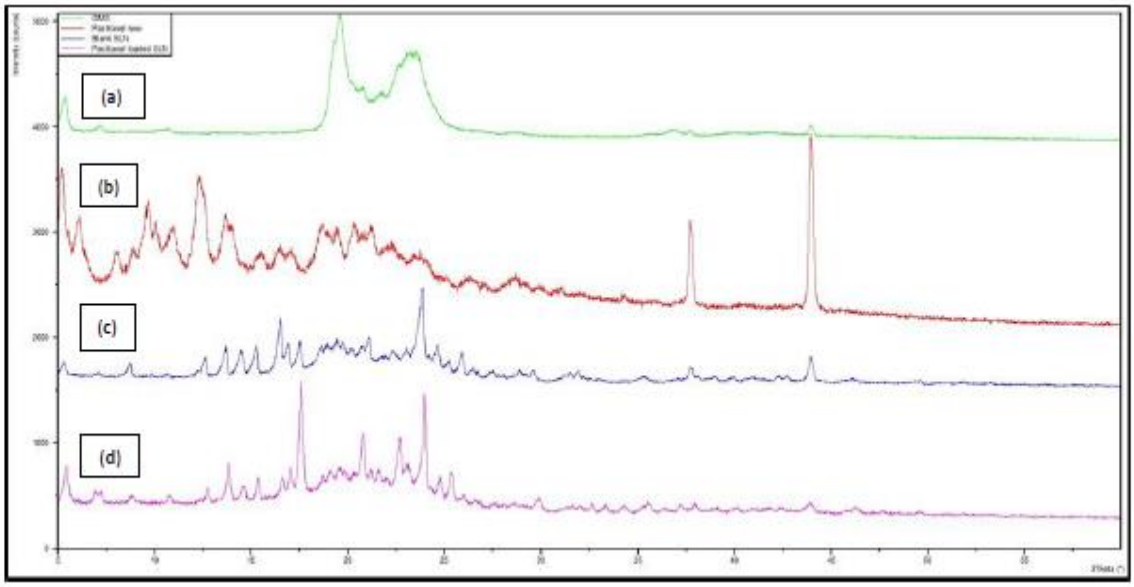

Figure 5: P-XRD patterns of (a) pure GMS (b) pure Paclitaxel (c) lyophilized blank SLNs (d) lyophilized paclitaxel loaded SLNs.

4.8. ATR-FTIR

FTIR analysis was conducted to investigate the structural composition of the SLNs. The spectrum obtained for the blank SLNs closely matched that of pure GMS (Figures 6a and 6c). The obtained spectra clearly exhibited absorption bands corresponding to OH stretching at 3495 cm^{-1}, C-H stretching at 2913 cm^{-1}, C=O stretching at 1729 cm^{-1}, and C-H bending at both 1470 cm^{-1} and 1177 cm^{-1}. PCTL-loaded SLNs exhibited the distinctive absorption bands characteristic of PCTL, including N-H stretching around 3495–3300 cm^{-1}, C=O stretching from the ester group at 1731 cm^{-1}, amide bond at 1645 cm^{-1}, ester bond stretching at 1243 cm^{-1}, as well as C-N stretching at 1316 cm^{-1}. Additional aromatic bond signals were observed at 1645 cm^{-1}, 1073 cm^{-1}, 966 cm^{-1}, and 708 cm^{-1}.[31], in addition to those associated with GMS (Figure 6d). The paclitaxel-loaded SLNs spectrum verifies PCTL entrapment in the lipid matrix. The absorbance peak at 1200–1350 cm^{-1} was used to evaluate solid lipids, as it reveals key details about CH_2 group conformation.[32] Pure GMS exhibited distinct peaks in the 1200-1350 cm^{-1} range, which is characteristic of its ordered and crystalline structure (Figure 6a). Broad peaks were observed for PCTL-loaded SLNs in the

same region, indicating a possible reduction in the degree of crystallinity of GMS (Figure 6d). This observation is consistent with data from DSC and P-XRD.

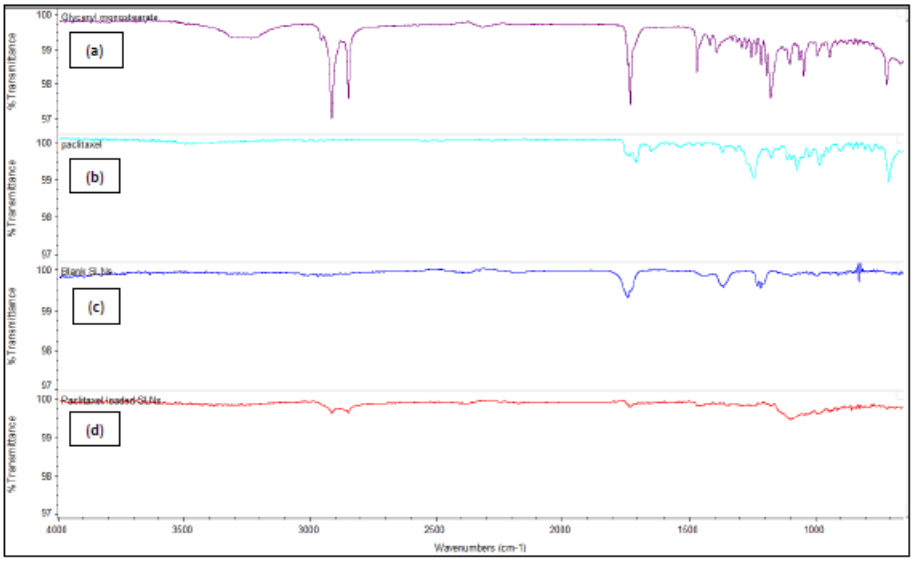

Figure 6: FTIR spectra of (a) pure GMS (b) pure PCTL (c) lyophilized blank SLNs, and (d) lyophilized PCTL-loaded SLNs.

4.9. Drug Entrapment Efficiency and Amount of Drug per mg of SLNs

To assess drug entrapment efficiency, lyophilized batches of both non-dialyzed and dialyzed SLNs containing 50 mg (50-N, 50-D), 75 mg (75-N, 75-D), and 100 mg (100-N, 100-D) of PCTL per mg of GMS were evaluated. The results indicated that drug entrapment was generally higher in non-dialyzed SLN batches than in dialyzed batches, with the exception of the 50 mg concentration (Figure 7). These findings indicate that the dialysis process results in the simultaneous loss of both the drug and the surfactant. Consequently, it is evident that incorporating the dialysis step adversely impacts the drug entrapment within the SLNs. The 50-N batch among the non-dialyzed samples had lower entrapment efficiency than the 75-N and 100-N batches (Figure 7). Both the 75-N and 100-N batches had similar entrapment efficiencies of about 62% (Figure 7). The PCTL content per milligram of SLNs was measured, and the 100-N batch demonstrated the highest value (Figure 8). As a result, the 100-N batch was selected as the formulation for subsequent studies. GMS was used as the lipid in this formulation. As a monoglyceride, GMS creates an ordered solid lipid matrix that reduces imperfections in the SLN structure. Consequently, the available space for drug molecules within the crystal lattice is decreased.[7]

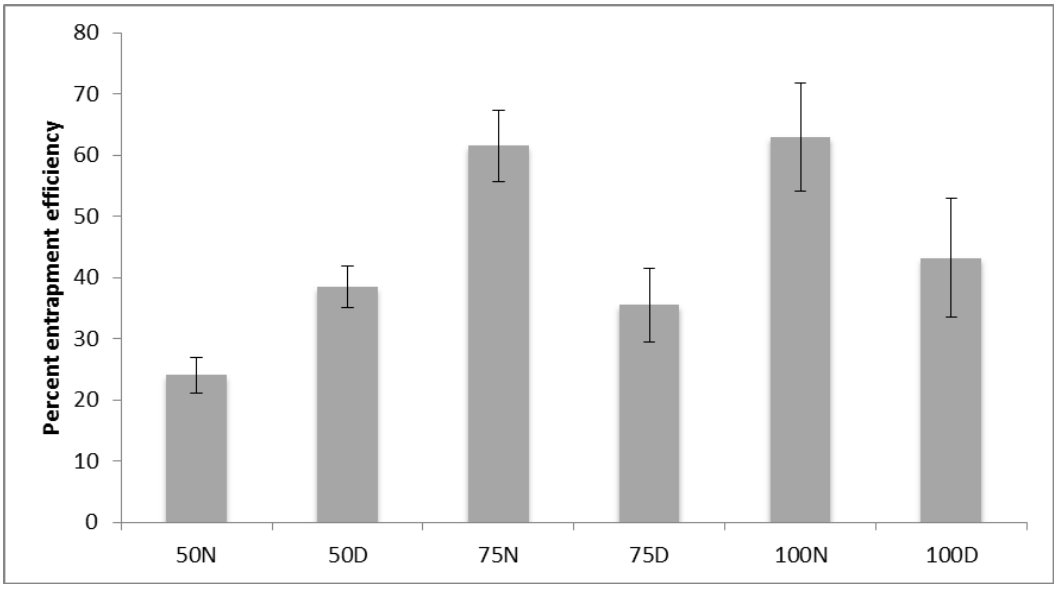

Figure 7: The entrapment efficiency of PCTL in SLNs. The data represent the mean values (n=3) ± S.E.

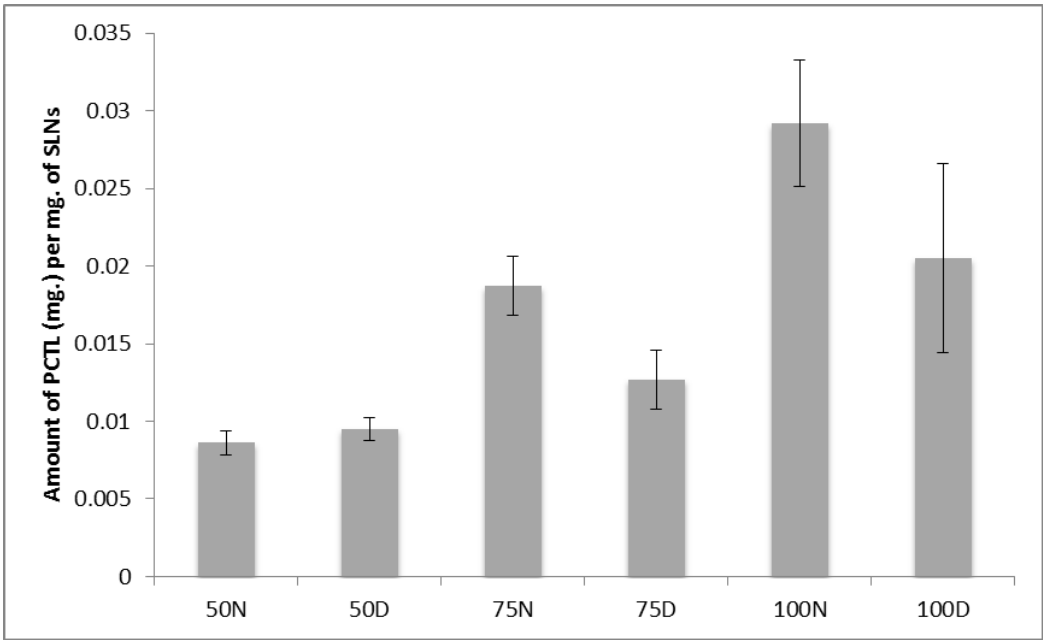

Figure 8: Amount of PCTL (mg) per mg of SLNs. The data represent the mean values (n=3) ± S.E.

4.10. In-vitro Drug Release Studies and Kinetic Modeling of the Drug Release Data

The in-vitro drug release profile of PCTL-loaded SLNs is presented in Figure 9. The SLNs demonstrated a biphasic release pattern, with an initial burst phase during the first 15 minutes releasing approximately 13% of the drug, followed by a sustained release over the course of one week. A maximum drug release of approximately 48% was achieved from the SLNs. Similar biphasic drug release profiles for SLNs have been reported by several other

researchers.[33-35] The observed release profile can be attributed to the partitioning behavior of the drug between the molten lipid phase and the aqueous phase during the homogenization stage of formulation. In this step, hot water is utilized and progressively cooled in an ice bath while homogenization is conducted simultaneously. As the water temperature decreases, the drug's solubility in water decreases, resulting in its repartitioning into the lipid phase. When the lipid reaches its recrystallization temperature, a solid core begins to form that incorporates the drug present within the lipid phase at that specific temperature. As the temperature continues to decrease, additional pressure is exerted on the drug to repartition into the lipid phase due to its further reduced aqueous solubility. Nevertheless, the pre-formed lipid core reaches its maximum drug capacity, resulting in an increased concentration of the drug in the outer shell or surface of the solid lipid nanoparticles (SLNs).[5] The sustained-release formulation of PCTL enables prolonged drug delivery, thereby decreasing the required frequency of administration. Analysis of the in-vitro release data demonstrated that the Higuchi model provided the best fit among the various kinetic models evaluated. (Table 4 and Figure 10c).

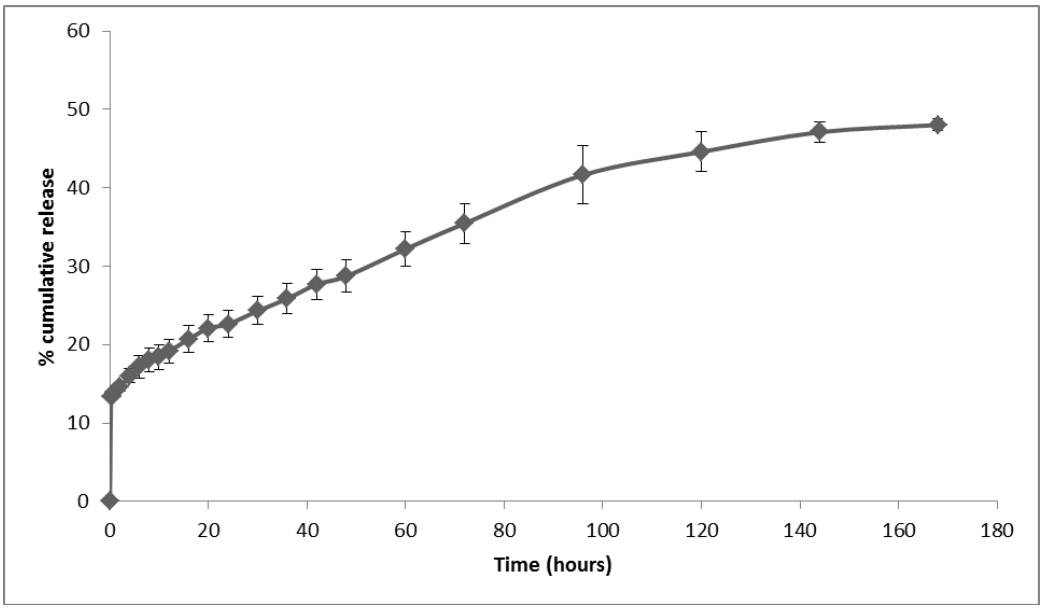

Figure 9: The in-vitro drug release profile of PCTL loaded SLNs. The data represent the mean values (n=3) ± S.E.

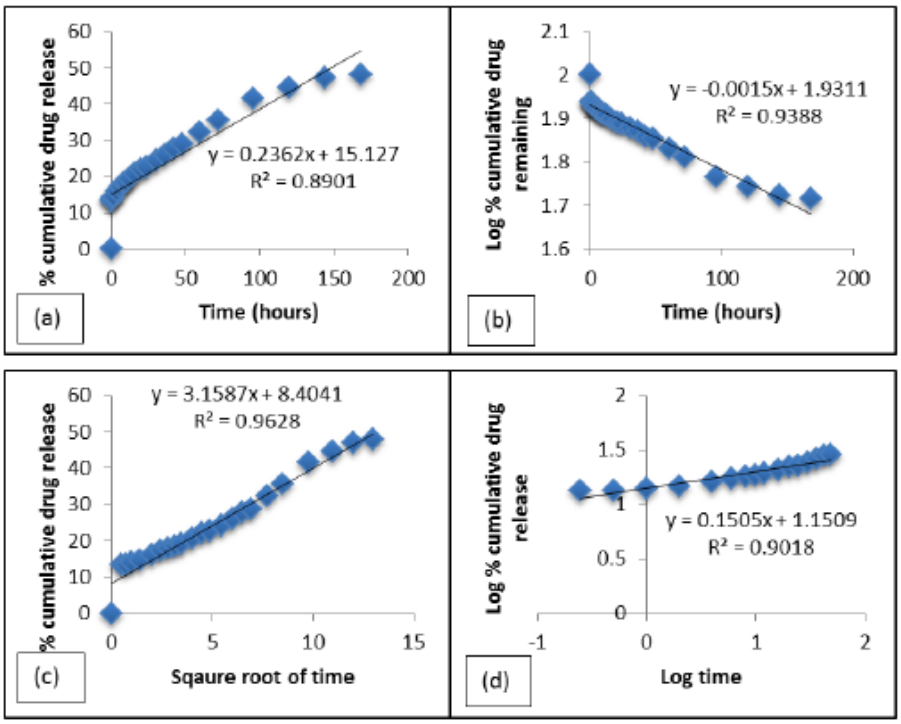

Figure 10: Kinetic model plots for (a) Zero order (b) First order (c) Higuchi and (d) Korsemeyer-Peppas model.

Table 4: Kinetic parameters of drug release data.

Kinetic models	R^2-value	k-value (hour^{-1})
Zero-order	0.89009	0.2362
First-order	0.93878	0.0006
Higuchi	0.96281	3.1587
Korsemeyer-Peppas	0.90181	14.1547

Analysis of the drug release data revealed that the Higuchi model provided the best fit, as indicated by the highest R^2 value (see Figure 10 and Table 4). Accordingly, the drug release from the SLNs is governed by Fickian diffusion, with the drug diffusing from the lipid matrix.

5. CONCLUSIONS

In this study, paclitaxel-loaded SLNs were formulated using a temperature-modulated solidification technique. Analysis of particle size by DLS and imaging with TEM indicated that the resulting nanoparticles were spherical and within the nanometer size range. AFM testing further validated the spherical morphology and nanoscale dimensions of the SLNs. Findings from DSC, P-XRD, and FTIR elucidated the solid-state properties and confirmed the successful entrapment of paclitaxel within the lipid matrix. Our preparation technique

resulted in approximately 62% of paclitaxel being entrapped within the nanoparticles. The in-vitro release studies demonstrated a sustained release of paclitaxel over one week. These findings indicate that the formulated nanoparticles have potential for use in anticancer therapy.

6. ACKNOWLEDGEMENTS

The authors would like to express their sincere gratitude to Dr. Joseph Lawrence for his assistance with the Transmission Electron Microscopy (TEM) studies and to Dr. Pannee Burckel for her support with the powder X-Ray Diffraction (p-XRD) studies. Appreciation is also extended to Dr. Steven Gollmer and Dr. Elisha Injeti for their contributions to the Atomic Force Microscopy (AFM) studies. The authors additionally thank Cedarville University, Ohio, USA, for granting access to their facilities for the AFM testing.

7. REFERENCES

1. Priyadarshini, K. and U.K. Aparajitha, Paclitaxel against cancer: a short review. Med chem, 2012; 2: 139-41.
2. Emami, J., M. Rezazadeh, and J. Varshosaz, Formulation of LDL targeted nanostructured lipid carriers loaded with paclitaxel: a detailed study of preparation, freeze drying condition, and in vitro cytotoxicity. Journal of Nanomaterials, 2012; 2012: p. 3.
3. Li, R., J.S. Eun, and M.-K. Lee, Pharmacokinetics and biodistribution of paclitaxel loaded in pegylated solid lipid nanoparticles after intravenous administration. Archives of pharmacal research, 2011; 34(2): p. 331-337.
4. A. Deshpande, M. Mohamed, S. B. Daftardar, M. Patel, S. H. S. Boddu, and J. Nesamony, "Solid Lipid Nanoparticles in Drug Delivery: Opportunities and Challenges," in Emerging Nanotechnologies for Diagnostics, Drug Delivery and Medical Devices, Elsevier Inc., 2017; pp. 291–330. doi: 10.1016/B978-0-323-42978-8.00012-7.
5. MuÈller, R.H., K. MaÈder, and S. Gohla, Solid lipid nanoparticles (SLN) for controlled drug delivery–a review of the state of the art. European journal of pharmaceutics and biopharmaceutics, 2000; 50(1): p. 161-177.
6. Mehnert, W. and K. Mäder, Solid lipid nanoparticles: production, characterization and applications. Advanced drug delivery reviews, 2001; 47(2): p. 165-196.
7. Lakkadwala, S., et al., Physico-chemical characterisation, cytotoxic activity, and biocompatibility studies of tamoxifen-loaded solid lipid nanoparticles prepared via a

temperature-modulated solidification method. Journal of microencapsulation, 2014; 31(6): p. 590-599.

8. Lee, M.-K., S.-J. Lim, and C.-K. Kim, Preparation, characterization and in vitro cytotoxicity of paclitaxel-loaded sterically stabilized solid lipid nanoparticles. Biomaterials, 2007; 28(12): p. 2137-2146.
9. Patel, M.N., et al., Characterization and evaluation of 5-fluorouracil-loaded solid lipid nanoparticles prepared via a temperature-modulated solidification technique. AAPS PharmSciTech, 2014; 15(6): p. 1498-1508.
10. Chen, D.-B., et al., In vitro and in vivo study of two types of long-circulating solid lipid nanoparticles containing paclitaxel. Chemical and pharmaceutical bulletin, 2001; 49(11): p. 1444-1447.
11. Silva, A., et al., Solid lipid nanoparticles (SLN)-based hydrogels as potential carriers for oral transmucosal delivery of Risperidone: Preparation and characterization studies. Colloids and Surfaces B: Biointerfaces, 2012; 93: p. 241-248.
12. Singhvi, G. and M. Singh, Review: in-vitro drug release characterization models. Int J Pharm Stud Res, 2011; 2(1): p. 77-84.
13. Zhang, J., Y. Fan, and E. Smith, Experimental design for the optimization of lipid nanoparticles. Journal of pharmaceutical sciences, 2009; 98(5): p. 1813-1819.
14. Heydenreich, A., et al., Preparation and purification of cationic solid lipid nanospheres—effects on particle size, physical stability and cell toxicity. International journal of pharmaceutics, 2003; 254(1): p. 83-87.
15. del Pozo-Rodríguez, A., et al., Short-and long-term stability study of lyophilized solid lipid nanoparticles for gene therapy. European Journal of Pharmaceutics and Biopharmaceutics, 2009; 71(2): p. 181-189.
16. Pardeshi, C., et al., Solid lipid based nanocarriers: An overview/Nanonosači na bazi čvrstih lipida: Pregled. Acta Pharmaceutica, 2012; 62(4): p. 433-472.
17. Yang, S.C. and J.B. Zhu, Preparation and characterization of camptothecin solid lipid nanoparticles. Drug development and industrial pharmacy, 2002; 28(3): p. 265-274.
18. Hu, L., et al., Preparation and enhanced oral bioavailability of cryptotanshinone-loaded solid lipid nanoparticles. AAPS PharmSciTech, 2010; 11(2): p. 582-587.
19. Liu, J., et al., Solid lipid nanoparticles loaded with insulin by sodium cholate-phosphatidylcholine-based mixed micelles: preparation and characterization. International journal of pharmaceutics, 2007; 340(1): p. 153-162.

20. Müller, R., C. Jacobs, and O. Kayser, Nanosuspensions as particulate drug formulations in therapy: rationale for development and what we can expect for the future. Advanced drug delivery reviews, 2001; 47(1): p. 3-19.
21. Kuntsche, J., J.C. Horst, and H. Bunjes, Cryogenic transmission electron microscopy (cryo-TEM) for studying the morphology of colloidal drug delivery systems. International journal of pharmaceutics, 2011; 417(1): p. 120-137.
22. Dubes, A., et al., Scanning electron microscopy and atomic force microscopy imaging of solid lipid nanoparticles derived from amphiphilic cyclodextrins. European journal of pharmaceutics and biopharmaceutics, 2003; 55(3): p. 279-282.
23. Zimmermann, E., E. Souto, and R. Müller, Physicochemical investigations on the structure of drug-free and drug-loaded solid lipid nanoparticles (SLNTM) by means of DSC and 1H NMR. Die Pharmazie-An International Journal of Pharmaceutical Sciences, 2005; 60(7): p. 508-513.
24. Radomska-Soukharev, A., Stability of lipid excipients in solid lipid nanoparticles. Advanced drug delivery reviews, 2007; 59(6): p. 411-418.
25. Li, Z., et al., Studies on crystallinity state of puerarin loaded solid lipid nanoparticles prepared by double emulsion method. Journal of thermal analysis and calorimetry, 2010; 99(2): p. 689-693.
26. Liggins, R.T., W. Hunter, and H.M. Burt, Solid-state characterization of paclitaxel. Journal of pharmaceutical sciences, 1997; 86(12): p. 1458-1463.
27. Cavalli, R., et al., Sterilization and freeze-drying of drug-free and drug-loaded solid lipid nanoparticles. International journal of pharmaceutics, 1997; 148(1): p. 47-54.
28. Rahman, Z., A.S. Zidan, and M.A. Khan, Non-destructive methods of characterization of risperidone solid lipid nanoparticles. European Journal of Pharmaceutics and Biopharmaceutics, 2010; 76(1): p. 127-137.
29. Hou, D., et al., The production and characteristics of solid lipid nanoparticles (SLNs). Biomaterials, 2003; 24(10): p. 1781-1785.
30. Feng, F., et al., Preparation, characterization and biodistribution of nanostructured lipid carriers for parenteral delivery of bifendate. Journal of microencapsulation, 2011; 28(4): p. 280-285.
31. Martins, K.F., et al., Preparation and characterization of paclitaxel-loaded PLDLA microspheres. Materials Research, 2014(AHEAD): p. 0-0.
32. Wunder, S.L. and S.D. Merajver, Raman spectroscopic study of the conformational order in hexadecane solutions. The Journal of Chemical Physics, 1981; 74(10): p. 5341-5346.

33. Shah, R.M., et al., Physicochemical characterization of solid lipid nanoparticles (SLNs) prepared by a novel microemulsion technique. Journal of colloid and interface science, 2014; 428: p. 286-294.
34. Xiang, Q.-y., et al., Lung-targeting delivery of dexamethasone acetate loaded solid lipid nanoparticles. Archives of pharmacal research, 2007; 30(4): p. 519-525.
35. Abbaspour, M., et al., Effect of anionic polymers on drug loading and release from clindamycin phosphate solid lipid nanoparticles. Tropical Journal of Pharmaceutical Research, 2013; 12(4): p. 477-482.